Giant quadrupole and monopole resonances in ^{28}Si

Y.-W. Lui, J. D. Bronson, D. H. Youngblood, and Y. Toba
Cyclotron Institute, Texas A&M University, College Station, Texas 77843

U. Garg*
Physics Department, University of Notre Dame, Notre Dame, Indiana 46556
and Cyclotron Institute, Texas A&M University, College Station, Texas 77843

(Received 25 January 1984)

Inelastic alpha scattering measurements have been performed for ^{28}Si at small angles including zero degrees. A total of 66% of the $E0$ energy-weighted sum rule was identified (using a Satchler version 2 form factor) centered at $E_x = 17.9$ MeV having a width of 4.8 MeV and 34% of the $E2$ energy-weighted sum rule was identified above $E_x = 15.3$ MeV centered at 19.0 MeV with a width of 4.4 MeV. The dependence of the extracted $E0$ strength on form factor and optical potential was explored.

INTRODUCTION

The properties of the giant monopole resonance (GMR) are of particular importance because the incompressibility of nuclei is directly related to the energy of the GMR. In order to obtain the incompressibility of nuclear matter, some extrapolation must be made from finite nuclei. These extrapolations have been done several ways. One method attempts to properly take into account the finite nucleus by calculating the energy of the GMR utilizing specific interactions, and calculating the infinite matter incompressibility with the interaction most closely reproducing experimental data.[1] Another uses the empirical relation

$$K_A = K_{\rm vol} + K_{\rm surf}(A^{-1/3}) + K_{\rm sym}[(N-Z)/A]^2 + K_{\rm Coul} , \quad (1)$$

which attempts to account for surface, symmetry, and Coulomb effects to obtain $K_{\rm vol}$, usually identified as the nuclear matter incompressibility $K_{\rm nm}$, from K_A for finite nuclei.[1,2] Whatever method is used, however, one has to relate the incompressibility of a finite nucleus to that of nuclear matter if the incompressibility of nuclear matter is to be obtained. While the GMR has been identified in a number of nuclei with $A \geq 90$, and approximately 30% of the GMR energy weighted sum rule (EWSR) has been identified in a concentrated resonance in ^{64,66}Zn, the GMR has not been identified for lighter nuclei. The accuracy of extrapolations would likely be improved if this state could be located in lighter nuclei.

There have been several studies of lighter nuclei attempting to locate the GMR. Lebrun *et al.*[3] studied the giant resonance region in ^{27}Al, ^{40}Ca, ^{56}Fe, and ^{58,60}Ni using inelastic scattering of 108.5 MeV ^{3}He particles at small angles and reported a small amount ($<10\%$ EWSR) of concentrated monopole strength situated close to the excitation energy of the giant quadrupole resonance (GQR). van der Borg *et al.*[4] have performed a detailed study of the isoscalar strength distributions in ^{24,26}Mg, ^{28}Si, and ^{40}Ca; they found a large amount of the $E2$ EWSR exhausted between 14 and 27 MeV, consistent with earlier studies by Youngblood *et al.*,[5] who investigated ^{24}Mg, ^{27}Al, and ^{28}Si with 126 MeV inelastic alpha scattering. Some evidence of $E0$ strength was also found; however, neither of these experiments was particularly sensitive to $J^\pi = 0^+$ strength nor were they able to definitively distinguish 0^+ from 2^+ due to the lack of data points at very forward angles. In their angular correlation measurements of α_0 decay from ^{40}Ca, Zwarts *et al.*[6] identified about 12% of the $E2$ strength between 12.5 and 15.5 MeV and, extrapolating to all channels, suggested the existence of 45% of the $E2$ EWSR in this region. Kailas *et al.*[7] showed that their inelastic proton scattering data on ^{28}Si can be explained by taking into account contributions from $L=0$, $L=1$, $L=2$, and $L=4$ in the giant resonance region. However, the $E0$ strength contribution necessary depends very much upon the contribution from the giant dipole resonance (GDR), which is not well determined. Recently, Brandenburg *et al.*[8] reported about 30% of $E0$ strength in ^{40}Ca between 10–20 MeV excitation from inelastic alpha scattering and charged particle decay coincidence measurements. In this paper we report small angle inelastic alpha scattering measurements on ^{28}Si which indicate that some substantial portion of the GMR EWSR is located in a concentrated peak at approximately 18 MeV excitation, somewhat below the giant quadrupole resonance.

EXPERIMENTAL PROCEDURE

Inelastically scattered spectra were measured for 129 MeV alpha particles obtained from the Texas A&M University variable energy cyclotron. The experimental setup and beam preparation methods were similar to those discussed in detail in Refs. 9 and 10. Considerable care was taken to minimize spurious contributions from the beam as well as slit scattering. Runs with blank target frames were taken to ascertain that contributions from such processes were negligible in regions of interest. The

thickness of the ^{28}Si target was 2.05 mg/cm^2. The inelastically scattered alpha particles were detected in the focal plane of the Enge split-pole spectrograph with a 40-cm long resistive wire proportional counter backed by an NE102 plastic scintillator. For the 0° measurement, the solid angle defining slits were open ±2.3° both horizontally and vertically, while for all nonzero angles they were set at ±0.3° horizontally and ±0.9° vertically. An active slit system was used to reduce slit scattering from the solid angle defining collimator. The system is similar to the one developed at Grenoble[11] and utilizes a thin plastic scintillator situated at the back of the solid angle defining collimator. The particles scattered from the edge of the collimator pass through the thin scintillator; the signals from the scintillator are in anticoincidence with the scintillator signals from the focal plane detector. Details of the electronic setup, the data acquisition system, background subtraction techniques, and the distorted wave Born approximation (DWBA) calculations are discussed in Ref. 10. Calculations were averaged over the finite angle opening of the detector. The isoscalar transition rates were calculated using a uniform matter distribution (UMD) as described by Bernstein.[10,12] Recently, Wagner *et al.*[13] applied an implicit folding procedure (IFP) to extract isoscalar transition rates for inelastic hadron scattering from light nuclei, and values obtained with this technique are also presented.

RESULTS AND DISCUSSION

Data were taken at nine angles between $\theta_{lab}=0°$ and 8.6° for ^{28}Si. The 0° data were extracted in a separate experiment measuring charged particle decay from the giant resonance (GR) region in ^{28}Si.[14] Sample ^{28}Si spectra are shown in Fig. 1. The yield in the hatched area in Fig. 1 is from scattering from the beam stop located just in front of the solid angle defining slit. Due to the appearance of this scattering (it was absent at larger angles and at 0°), this is the most forward nonzero degree angle measured. The background-subtracted spectra for $\theta_{lab}=0°$ and 4.6° are shown in Fig. 2. The distinct difference between the 0° and 4.6° spectra in the GR region provides a clear signature for the presence of substantial concentrated monopole strength in this nucleus.

The angular distributions of the 3^- states at 6.88 and 10.17 MeV are shown in Fig. 3 along with DWBA calculations. The 0° point for the 10.17 MeV state is not included because the state is too close to the 0° beam stop for reliable extraction. The optical potentials used for these calculations were those for ^{27}Al reported in Ref. 5. The DWBA calculations for these states are in good agreement with the experimental data. Preliminary analysis indicates no significant monopole strength below 15.3 MeV; therefore detailed analysis was carried out only for $E_x \geq 15.3$ MeV. Analysis of the data in the region between 15.3 and 24.7 MeV were done by integrating the resolved fine structure. The angular distributions obtained are also shown in Fig. 3 where the error bars on the differential cross section represent not only the statistical error but also the uncertainties in the integrating process and background subtraction. The groups at 18.7, 19.8,

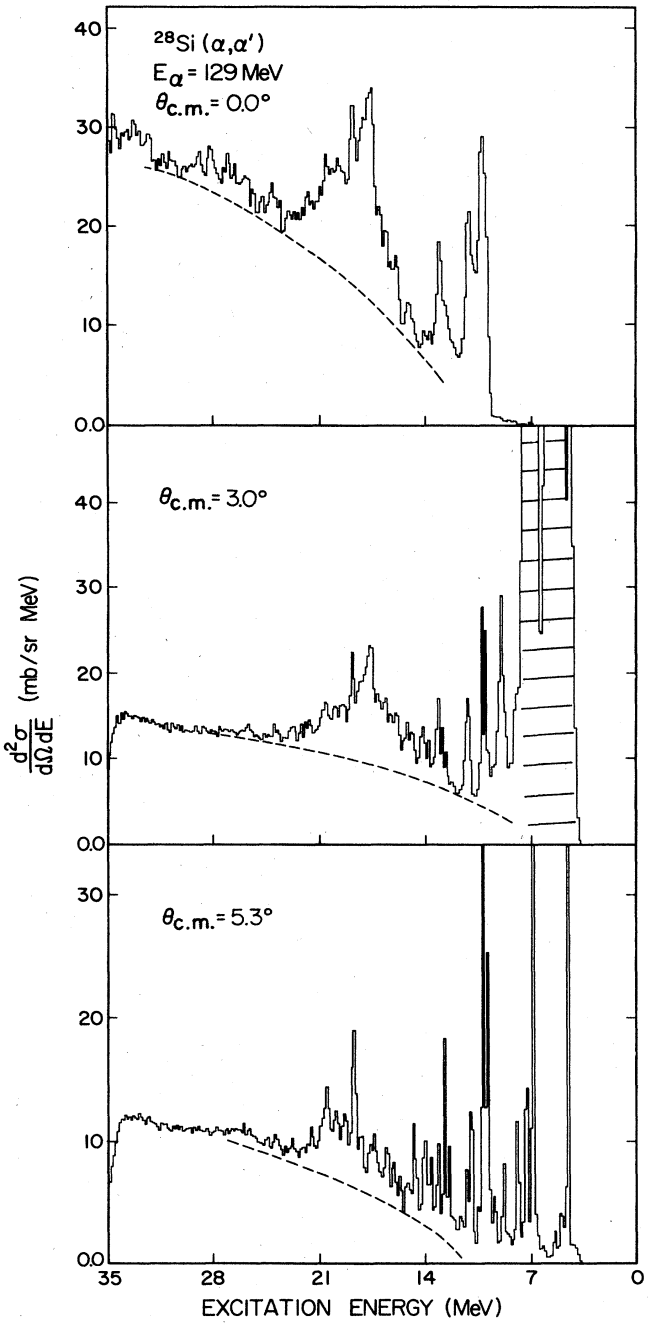

FIG. 1. Energy spectra of ^{28}Si at 0°, 3.0°, and 5.3°. The dashed lines represent the assumed shape of the underlying continuum subtracted as background for analysis. The hatched area in the 3° spectrum is slit scattering (see the text).

and 20.5 MeV are fit reasonably well by an $L=2$ DWBA calculation; however, the rest are not fit well by calculations for any one multipolarity. In particular, the rise in cross section at very forward angles for most of the groups indicates the presence of some $L=0$ strength.

In order to ascertain what L values are contributing to each region, the angular distributions (excluding the 0° point) for all of the regions were fit by a combination of

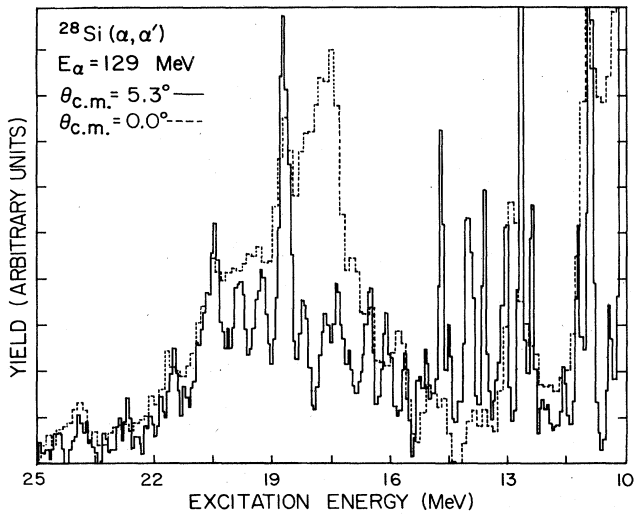

FIG. 2. Background subtracted spectra of ^{28}Si at 0° and 5.3°.

$L=0$, 2, 3, and 4 distributions calculated in DWBA, using a least squares technique to determine the contribution of each multipolarity. Since the isovector dipole should be at most very weakly excited in these alpha scattering experiments, no $L=1$ contribution was included. The technique used to determine the number of multipolarities contributing was as follows. Each angular distribution was fit successively with one, two, three, and four multipolarities to determine which combination produced a significant minimum in χ^2. In general it was found that some combination of two multipolarities produced a low χ^2, with the addition of other multipolarities having only a small effect. The fit that produced a low χ^2 with the least contributing multipolarities was then chosen as the most likely. These results are shown in Table I, where some representative combinations used and the χ^2 values obtained are listed. For example, for the group centered at 16.6 MeV the calculation using 0^+, 2^+, and 4^+ gives essentially the same χ^2 as the calculation using 0^+ and 2^+, while other combinations give significantly larger χ^2 values. For the 19.8 MeV group, the calculation with only 2^+ gives a χ^2 value comparable to calculations using 0^+ and 2^+ and 0^+, 2^+, and 4^+. In fitting the angular distribution of the summed region between 15.3 and 18.3 MeV, the χ^2 value obtained using the sum of 0^+, 2^+, and

TABLE I. Results of fits with differing L contributions.

E_x (MeV)	No. of L values	J^π	χ^2
16.6	3	$0^+,2^+,4^+$	1.9
	2	$0^+,2^+$	2.0
	1	0^+	32.6
	1	2^+	6.9
17.7	2	$0^+,3^-$	18.6
	2	$0^+,2^+$	8.1
	1	0^+	30.1
	1	2^+	15.9
19.8	3	$0^+,2^+,4^+$	0.6
	2	$0^+,2^+$	0.6
	1	0^+	41.7
	1	2^+	0.7
15.3–18.3	3	$0^+,2^+,4^+$	0.5
	2	$0^+,2^+$	1.2
	2	$0^+,4^+$	15.3
	2	$2^+,4^+$	8.8
	1	0^+	33.1
	1	2^+	9.1
	1	3^-	13.3
	1	4^+	30.7

TABLE II. J^π assignments and EWSR strengths obtained for ^{28}Si.

E_x (MeV)	J^π	EWSR (%)	χ^2
15.7	0^+	4.9 ±0.4	1.4
	2^+	0.51±0.05	
16.1	0^+	0.6 ±0.4	4.4
	2^+	1.42±0.09	
16.6	0^+	4.1 ±0.7	2.0
	2^+	1.56±0.11	
17.0	0^+	3.9 ±0.4	8.4
	2^+	0.76±0.05	
17.4	0^+	4.3 ±1.0	10.2
	2^+	2.14±0.14	
17.7	0^+	7.9 ±1.0	8.1
	2^+	1.52±0.12	
18.2	0^+	8.9 ±1.0	1.4
	2^+	1.92±0.14	
18.7	2^+	6.3 ±0.2	1.4
19.3	0^+	3.0 ±1.3	1.4
	2^+	3.4 ±0.2	
19.8	2^+	3.84±0.14	0.7
20.5	2^+	5.9 ±0.2	2.8
21.6	0^+	6.8 ±1.7	1.7
	2^+	3.1 ±0.2	
	4^+	0.6 ±0.2	
22.7	0^+	8.9 ±1.1	2.4
	2^+	1.63±0.11	
15.3–18.3	0^+	39 ±5	1.2
	2^+	9.1 ±0.7	
18.3–23.0	0^+	20 ±9	0.7
	2^+	22.7 ±1.4	
23.3–24.7	0^+	6.5 ±1.4	1.3
	2^+	2.32±0.15	

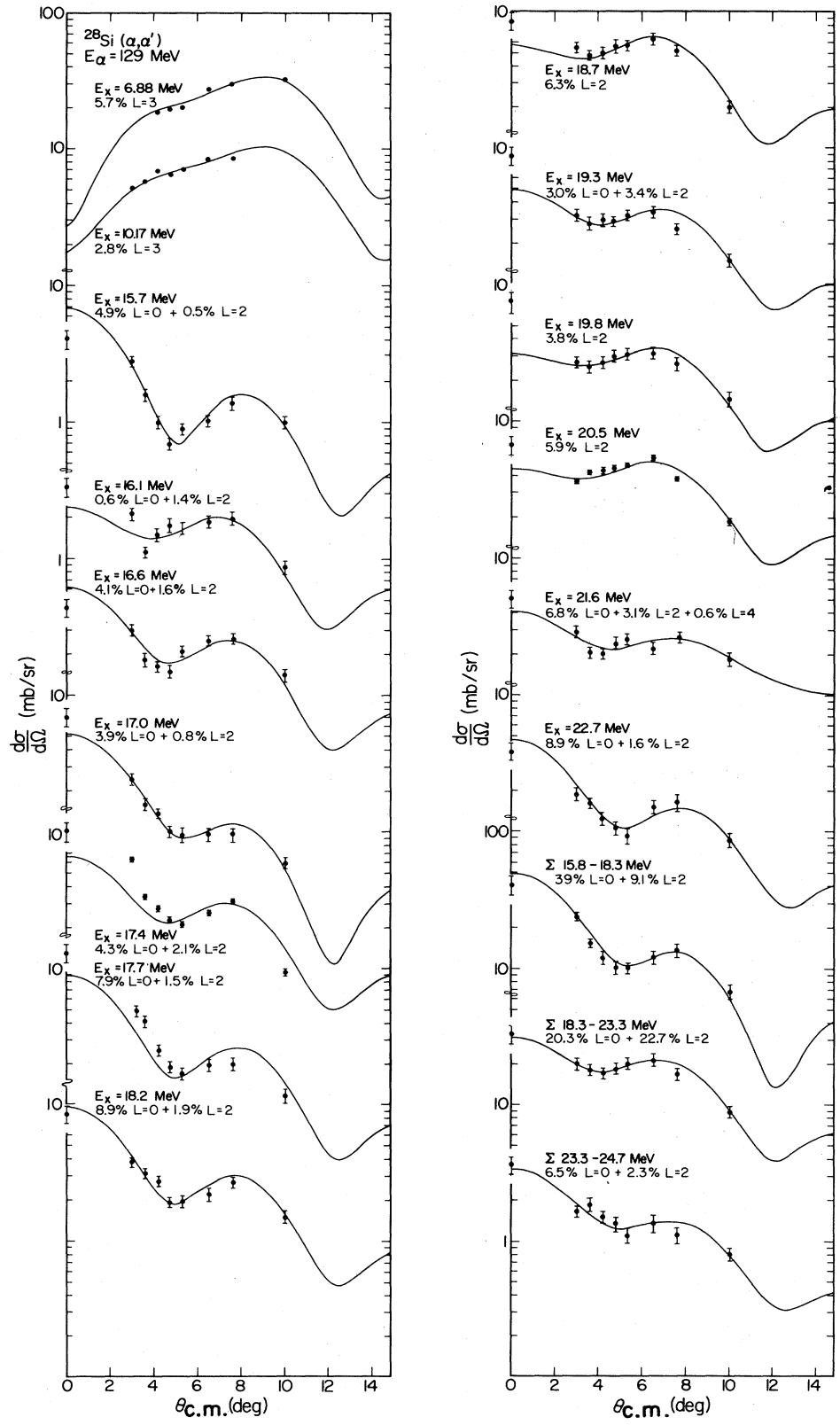

FIG. 3. Angular distributions obtained for the 6.88 MeV state, the 10.17 MeV state, and the fine structures in the GR region of ^{28}Si. The curves are summed DWBA calculations for the L transfers indicated. The error bars indicate statistical and background errors only. The 0° points are not raw data. Their evolution is discussed in the text.

4^+ modes is slightly better than the sum of 0^+ and 2^+ modes; nevertheless, the $E4$ EWSR contribution is small with relatively large error. The fit using the sum of 0^+ and 2^+ modes gave a χ^2 value much smaller than calculations with any one multipolarity or with any other two multipolarities. In general, the fits to the angular distributions in the region between 15.3 and 24.7 MeV gave contributions from $L=3$ and $L=4$ modes which were considerably less than the errors on the contributions, and the inclusion of these only slightly improved the χ^2 value, so most of the fits chosen contain $L=0$ and $L=2$ contributions only.

The J^π assignments and the EWSR values obtained with the UMD for the structures in the GR region from the least square fits are listed in Table II. Also listed are the uncertainties in the strength of each contribution obtained from the least square fits and the χ^2 values for each fit. The uncertainties listed do not include systematic errors, but include statistical uncertainties, uncertainties in picking backgrounds, and uncertainties in the least square fitting process.

The 0° data were taken with a substantially different solid angle and the points shown have been renormalized to adjust to the same solid angle as the other data points, assuming the mix of multipolarities indicated for each state (obtained from fitting data excluding the 0° point) and an angular averaging appropriate for the solid angle using the calculated angular distributions. The renormalization was designed to yield data points which should be correct for small solid angle data taken at 0° with the mix of multipolarities indicated for each state.

Table III shows the isoscalar transition rates, G(IS), for low lying 2^+ and 3^- states from inelastic alpha scattering and the corresponding electromagnetic transition rates G(EM). For comparison purposes values calculated with the uniform matter distribution are compared to those calculated with a Fermi distribution and those with an IFP. For the 1.78 MeV 2^+ state, the isoscalar transition rate obtained using the uniform matter distribution averaged over the three experiments[16,5,4] is approximately 30% smaller than the electromagnetic transition value, while the isoscalar value is about one-third the electromagnetic value for the 6.88 MeV 3^- state. The IFP brings the isoscalar rate for the 3^- state into agreement with the electromagnetic values, but for the 2^+ state the average G(IS) obtained is 29% higher than the electromagnetic value. The Fermi distribution results in isoscalar values below the electromagnetic values in both cases.

The $E0$ EWSR percentages listed in Table II were obtained by employing the collective model with the "version 2" (SV2) form factor for the GMR suggested by Satchler.[17] At least two other macroscopic form factors have been suggested for the GMR, viz., Satchler version 1 (SV1) (Ref. 17) and one by Kishimoto (KV).[18] These form factors correspond to different physical pictures for the $L=0$ vibrations and, in general, lead to predictions of very different cross sections. SV1 assumes the oscillation to be a compressional mode which leads to a form factor given by

$$U_1(r)=-3U_0(r)-r\frac{dU_0(r)}{dr} .$$

SV2, on the other hand, takes the surface of the nuclear matter distribution to be deformed as $R'=R(1+\alpha)$ and is closer to the standard prescription for higher multipoles. The SV2 form factor is

$$U_1(r)=-XU_0(r)-R\frac{dU_0(r)}{dr} ,$$

where

$$X=[3+(\pi a/R)^2]/[1+(\pi a/R)^2] .$$

KV follows an entirely different approach and employs a rigourous self-consistency between the density distribution and the potential resulting in a form factor given by

$$U_1(r)=\left[\frac{3}{r\langle r^{-2}\rangle}-r\right]\frac{dU_0}{dr} .$$

In all the above expressions, $U_0=V+iW$ is an appropriate optical model potential with radius R and diffuseness a, respectively. The ratio of DWBA cross section for GMR in ^{28}Si at 17.9 MeV using SV1, SV2, and KV form

TABLE III. Isoscalar and electromagnetic transition rates for low lying ^{28}Si levels. G(IS) values are given for three models (see Bernstein, Ref. 12).

E_x (MeV)	J^π	G(IS) Fermi	G(IS) Uniform	G(IS) IFP	G(EM)	Ref.
1.78	2^+	8.8[a]	6.5	13.1[c]	12.6±0.4[d]	16
		13.6	11.2	18.9		5
		10.3[b]	9.0	16.8[c]		4
6.88	3^-	4.8[b]	3.3	13.4[c]	12.3±1.9[d]	4
		5.8	3.5	11.2[e]		

[a]Original authors did not include an imaginary term in the form factor. The value presented here was adjusted to include the imaginary term with the assumption that $\beta_{\text{real}}=\beta_{\text{imag}}$.
[b]Values were calculated with the assumption that $\beta_{\text{real}}=\beta_{\text{imag}}$.
[c]Values were taken from analysis reported in Ref. 13.
[d]Reference 15.
[e]Using experimental data from present work and technique described in Ref. 13 to calculate isoscalar transition rate.

TABLE IV. Isoscalar multipole strength observed in GR region of ^{28}Si.

Reaction	Beam energy (MeV)	Excitation energy (MeV)	J^π	EWSR (%)	Ref.
(e,e′)	92	12–20	2^+	20±4	19
^{24}Mg(α,γ)		14.5–21.5	2^+	14.5	20
		14–22	2^+	~34	21[a]
(p,p′)	61	17–22	2^+	30	22
	115	15.7–24.1	0^+	34±33	7
			2^+	19±3	
			3^-	1.5±1.5	
			4^+	8±2	
(α,α')	120	14–25	0^+	4.5	4
			2^+	25^{+9}_{-4}	
			3^-	0.9±0.6	
	126	17–22	2^+	25	5
	129	15.3–24.7	0^+	66±20	Present work (UMD)
			2^+	34±6	
	155	16.9–24.8	2^+	31^{+8}_{-5}	16

[a]An EWSR was calculated assuming 11% of $E2$ decay through the α_0 channel.

factors is 4.5, 1.0, and 3.2, respectively. In the alpha and ^{3}He inelastic scattering studies of the GMR, most previous authors have used SV1 (the "breathing mode"), probably at least in part because SV2 gives a much lower cross section and would lead to GMR EWSR's considerably exceeding 100% in heavier nuclei. The "breathing mode," however, may not be appropriate for light mass nuclei.

Using UMD, 66% $E0$ EWSR is obtained with SV2 and 15% $E0$ EWSR is obtained with SV1. If IFP is used, somewhat different values are obtained, 51% of the $E0$ EWSR and 36% with SV1. Thus IFP brings SV1 and SV2 into closer agreement. However, if SV2 is appropriate, approximately half to two-thirds of the $E0$ EWSR is concentrated in this 9 MeV wide region. Use of the IFP for the $E2$ calculation yields a value of 44% for the total $E2$ strength between 15.3 and 24.7 MeV instead of the 34% obtained in the uniform matter assumption.

The isoscalar multipole strength observed in the present work is compared to other experiments in Table IV. In general, the $E2$ strength observed is in reasonable agreement with that reported from other experiments. The $E0$ strength agrees with that reported in Ref. 7 (within their large error), but it is considerably larger than that reported in the experiments described in Ref. 4. This discrepancy may be due in part to the lack of very small angle data ($\theta_{lab} < 6°$) in the experiments described in Ref. 4, since the $E0$ strength shows most clearly at smaller angles. Additionally, the differing optical potentials used in the present work and Ref. 4 result in some differences in strength (5% difference in EWSR for $E2$, and 29% difference for $E0$ strength with SV2 form factor and UMD).

The distributions of $E0$ and $E2$ EWSR strengths between 15.3 and 24.7 MeV are shown in Fig. 4. The $E0$

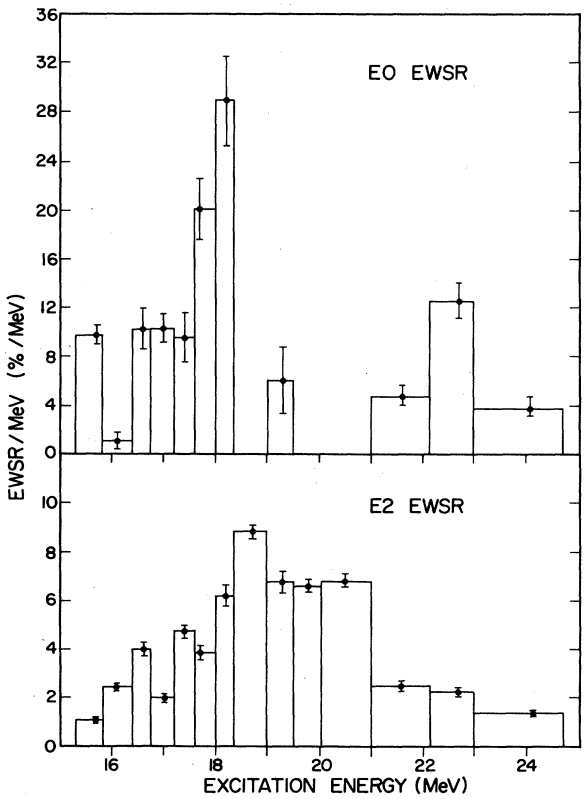

FIG. 4. Distributions of $E0$ and $E2$ energy weighted sum rule strength between 15.3 and 24.7 MeV in ^{28}Si from the present experiment. The error bars shown correspond to the uncertainties given in Table II. The histogram represents the region of integration and the data points are plotted in EWSR per MeV at the centroid of each integration region.

TABLE V. Incompressibility parameters obtained (MeV).

	a	b
K_{vol}	270±13	221±32
K_{surf}	−607±43	−398±135
K_{sym}	−550±195	−285±253

[a]Including K_A values for ^{28}Si, ^{64,66}Zn, ^{112,116,118,120,124}Sn, ^{115}In, ^{142}Nd, ^{144}Sm, ^{197}Au, and ^{208}Pb.
[b]As for a without ^{28}Si.

EWSR distribution can be separated into two groups while the $E2$ EWSR distribution forms one broad peak. Integrating the region shown, the centroids of the $E0$ and $E2$ strength are obtained at 17.9±0.3 and 19.03±0.13 MeV, respectively, and the corresponding ($\Gamma_{FWHM} = 2.35 \times \Gamma_{rms}$) widths are 4.8 MeV and 4.4 MeV. In contrast to the heavier nuclei, the GMR is substantially below the GQR and corresponds in excitation to about $54A^{-1/3}$ MeV, whereas in heavier nuclei it lies at about $80A^{-1/3}$ MeV. The GQR, by contrast, is at $58A^{-1/3}$ MeV in ^{28}Si and $64A^{-1/3}$ MeV in ^{208}Pb.

The incompressibility parameters in Eq. (1) were obtained by a least square fit to the values of K_A obtained for 13 nuclei using the values reported in Refs. 9, 4, and 23 in addition to that for ^{28}Si. The fit assumed errors on GMR energy as reported by the authors. The results obtained are shown in Table V compared to those obtained without the ^{28}Si point. The addition of ^{28}Si significantly increases each of the parameters, with K_{vol} increasing from 221±32 to 270±13 MeV. This change is somewhat outside the combined uncertainties, obtained assuming the observed peak in each nucleus represents the entire GMR strength.

Figure 5 shows $EA^{1/3}$ vs A for a number of nuclei and includes results of random phase approximation (RPA) calculations by Blaizot *et al.*[1] with various effective interactions as well as a collective model prediction by Panharipande.[2] The trend of the data is somewhat different from the RPA calculations, with the actual monopole energy decreasing faster as A decreases than the calculations predict; however, the data are in good agreement with the collective model. The assumption that the entire GMR strength is contained in the observed peak is, of course, questionable, since using SV1 for the form factor and a uniform matter distribution, the three lowest mass points (28, 64, and 66) exhaust, respectively, only 15%, 29%, and 30% of the EWSR. On the other hand, with SV2 and a uniform matter distribution, these values change to 66%, 91%, and 92% of the EWSR, respectively. If, in fact, significant portions of the GMR lie unobserved at higher excitation in the lighter nuclei, the above extrapolations would be incorrect.

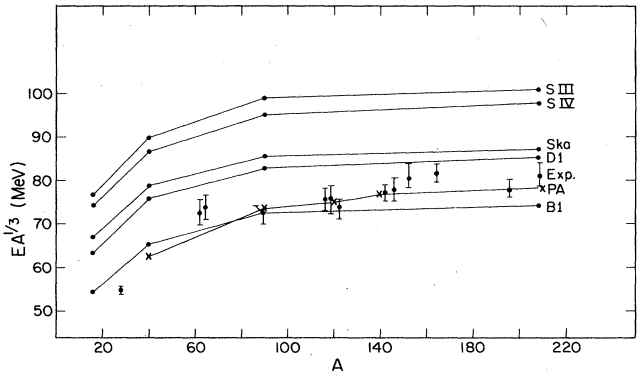

FIG. 5. Plot of $EA^{1/3}$ vs A for the GMR in several nuclei. Also shown are RPA predictions (Ref. 1) (solid lines) and a collective model prediction (Ref. 2) (PA).

It is important to perform microscopic RPA calculations to determine the nature of the form factor for the GMR. It is possible that the situation with the GMR is similar to that with the giant dipole resonance where the Goldhaber-Teller model works well for the light nuclei and the Steinwedel-Jensen model describes the GDR more appropriately for the medium- and heavy-mass nuclei. A form factor that is essentially a linear combination of the two has been proposed by Myers *et al.*[24] In a similar fashion, the SV2 form factor might be more appropriate for the GMR in light nuclei ($A < 40$), whereas SV1 is applicable in the medium- and heavy-mass region ($A > 90$). Clearly, a better understanding of the volume and surface effects regarding the GMR is needed.

ACKNOWLEDGMENTS

We are grateful to Dr. S. Shlomo for discussions on the relevant form factors. We would also like to thank M. Parkin for his assistance in taking data. This work was supported in part by the Department of Energy, the National Science Foundation, and The Robert A. Welch Foundation.

*Permanent address: Physics Department, University of Notre Dame, IN 46556.

[1]J. P. Blaizot, D. Gogny, and B. Grammaticos, Nucl. Phys. **A265**, 315 (1976).
[2]V. R. Pandharipande, Phys. Lett. **31B**, 635 (1970).
[3]D. Lebrun, M. Buenerd, P. Martin, P. de Saintegnon, and G. Perrin, Phys. Lett. **97B**, 358 (1980).
[4]K. van der Borg, M. N. Harakeh, and A. van der Woude, Nucl. Phys. **A365**, 243 (1981).
[5]D. H. Youngblood, C. M. Rozsa, J. M. Moss, D. R. Brown, and J. D. Bronson, Phys. Rev. C **15**, 1644 (1977).
[6]F. Zwarts, A. G. Dreutje, M. N. Harakeh, and A. van der Woude, Phys. Lett. **125B**, 123 (1983).
[7]S. Kailas, P. P. Singh, A. D. Bacher, C. C. Foster, D. L. Friesel, P. Schwandt, and J. Wiggins, Phys. Rev. C **25**, 1263 (1982).
[8]S. Brandenburg, R. De Leo, A. G. Drentje, M. N. Harakeh, H. Sakai, and A. van der Woude, Phys. Lett. **130B**, 9 (1983).
[9]D. H. Youngblood, P. Bogucki, J. D. Bronson, U. Garg, Y.-W. Lui, and C. M. Rozsa, Phys. Rev. C **23**, 1997 (1981).
[10]C. M. Rozsa, D. H. Youngblood, J. D. Bronson, Y.-W. Lui, and U. Garg, Phys. Rev. C **21**, 1252 (1980).

[11]M. Buenerd, C. Bonhomme, D. Lebrun, P. Martin, J. Chauvin, G. Duhamel, G. Perrin, and P. de Saintesnon, Phys. Lett. **84B**, 305 (1979).
[12]A. M. Bernstein, Adv. Nucl. Phys. **3**, 325 (1969).
[13]G. J. Wagner, P. Grabmayr, and H. R. Schmidt, Phys. Lett. **113B**, 447 (1982).
[14]Y.-W. Lui, P. Bogucki, J. D. Bronson, U. Garg, P. Grabmayr, K. T. Knopfle, H. Riedesel, G. J. Wagner, and D. H. Youngblood (unpublished).
[15]P. M. Endt and C. van der Leun, Nucl. Phys. **A310**, 1 (1978).
[16]K. T. Knopfle, G. J. Wagner, A. Kiss, M. Rogge, C. Mayer-Boricke, and Th. Bauer, Phys. Lett. **64B**, 263 (1976).
[17]G. R. Satchler, Part. Nucl. **5**, 105 (1973); Nucl. Phys. **A195**, 1 (1972).
[18]T. Kishimoto (unpublished).
[19]R. Pitthan, F. R. Buskirk, J. N. Dyer, E. E. Hunter, and G. Pozinsky, Phys. Rev C **19**, 299 (1979).
[20]S. S. Hanna, in *Lecture Notes in Physics 61,* Proceedings of the International School of Electro- and Photonuclear Reactions, edited by S. Costa and C. Schaerf (Springer, Berlin, 1977).
[21]E. Kuhlmann, K. A. Snover, G. Feldman, and M. Hindi, Phys. Rev. C **27**, 948 (1983).
[22]F. E. Bertrand, Annu. Rev. Nucl. Sci. **26**, 457 (1976).
[23]D. Lebrun, M. Buenerd, P. Martin, C. Bonhomme, J. Chauvin, G. Perrin, and P. de Saintesnon, in *Giant Multipole Resonances,* edited by F. E. Bertrand (Harwood, New York, 1980), p. 452.
[24]W. D. Meyers, W. J. Swiatecki, T. Kodama, L. J. El-Jaick, and E. R. Hilf, Phys. Rev. C **15**, 2032 (1977).